

Autonomous Intelligent Cruise Control

Petros A. Ioannou, *Member, IEEE*, and C. C. Chien

Abstract— Vehicle following and its effects on traffic flow has been an active area of research. Human driving involves reaction times, delays, and human errors that affect traffic flow adversely. One way to eliminate human errors and delays in vehicle following is to replace the human driver with a computer control system and sensors.

The purpose of this paper is to develop an autonomous intelligent cruise control (AICC) system for automatic vehicle following, examine its effect on traffic flow, and compare its performance with that of the human driver models. The AICC system developed is not cooperative; i.e., it does not exchange information with other vehicles and yet is not susceptible to oscillations and “slinky” effects. The elimination of the “slinky” effect is achieved by using a safety distance separation rule that is proportional to the vehicle velocity (constant time headway) and by designing the control system appropriately. The performance of the AICC system is found to be superior to that of the human driver models considered. It has a faster and better transient response that leads to a much smoother and faster traffic flow. Computer simulations are used to study the performance of the proposed AICC system and analyze vehicle following in a single lane, without passing, under manual and automatic control. In addition, several emergency situations that include emergency stopping and cut-in cases were simulated. The simulation results demonstrate the effectiveness of the AICC system and its potentially beneficial effects on traffic flow.

I. INTRODUCTION

URBAN highways in most major cities are congested and need additional capacity. Historically, capacity has been added and the congestion problem solved by building new highways. Unfortunately, adding highways is not a viable solution in many urban areas for a number of reasons: lack of suitable land, escalating construction costs, environmental considerations, etc. Because of these and other constraints, different ways to increase capacity must be found. One possible way to improve capacity is to use current highways more efficiently by removing as much human involvement as possible from the system through computer control and automation. In addition to capacity, automation may make driving and transportation in general safer, if designed properly.

The purpose of this paper is to examine the potential effects of partially automated vehicles on vehicle following in a single lane with no passing by comparing automatic and human driving responses. The automation considered is based on the so-called Autonomous Intelligent Cruise Control (AICC) or adaptive cruise control system [8] that several automobile companies are in the process of developing. In

such a system, the throttle and brake are controlled by the computer, and only steering is under manual control. The sensor on board of the vehicle senses relative distance and velocity of the immediate vehicle in front, and the computer control system sends the appropriate commands to the throttle and brake.

We propose a control law for an AICC system based on a constant time headway safety distance that we calculated using a reasonable worst-case stopping scenario. We investigated the properties of the control law for automatic vehicle following in a single lane with no passing under the assumption that all vehicles in the lane are using the same automatic feature. Due to the lack of exchange of information among vehicles, vehicle following may experience oscillations and slinky effects in the responses of intervehicle spacings, velocities, and accelerations as indicated in [1], [2], [11]. In our approach, slinky effects are theoretically totally eliminated, and oscillations are considerably suppressed. We considered a constant time headway separation rule that gave us an additional degree of freedom to design the AICC system to meet the specifications of no slinky effects and smaller oscillations without requiring any communication between vehicles.

Automatic vehicle following using the AICC system is compared with that of three human driver models proposed in the literature [2]–[6]. We use simulations to compare transient responses and steady state performance and their effects on traffic flow. The slinky effects, oscillations, and long settling times observed with the human driver models are non-existent in automatic vehicle following. Automatic vehicle following leads to smoother traffic flows and larger traffic flow rates due to the shorter inter-vehicle safety spacings used and the elimination of human delays and large reaction times. We simulated several emergency situations that included emergency stopping, cut-in, and exiting cases. During emergency stopping, the lead vehicle was assumed to decelerate with maximum deceleration of about 0.8 g, until it came to a full stop from 60 m.p.h (26.67 m/s). In this case, all vehicles followed the stopping maneuver and came to a full stop without collision. Cut-in situations where a vehicle under manual control cuts between vehicles under automatic control were also simulated, and the situations where collisions are possible are identified.

The paper is organized as follows: In Section II three human driver models that have been proposed in literature are reviewed. The safety distance policy, vehicle model, and longitudinal control laws proposed are given in Section III. In Sections IV and V the results of a series of simulations performed using a digital computer are presented and

Manuscript received September 1992; revised October 1992.

The authors are with the Southern California Center for Advanced Transportation Technologies, Department of Electrical Engineering, Systems, University of Southern California, Los Angeles, CA 90089-2562.

IEEE Log Number 9211462.

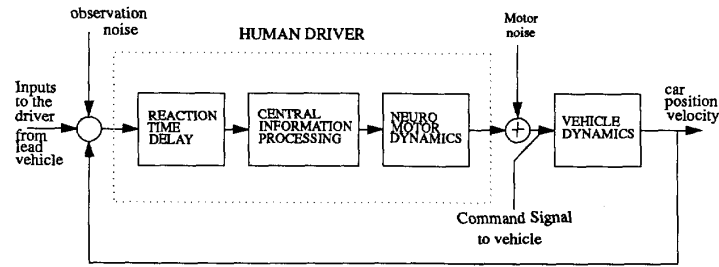


Fig. 1. Structure of the human driver mode.

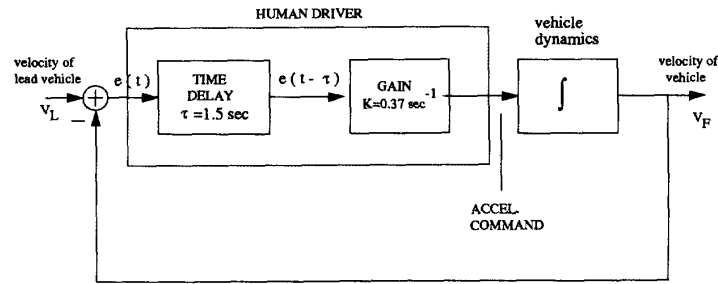


Fig. 2. Linear follow-the-leader model (Pipes model).

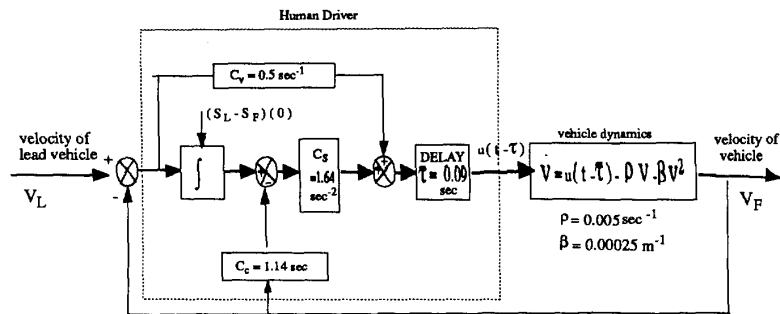


Fig. 3. Linear optimal control mode.

discussed. Some concluding remarks are given in Section VI.

II. MANUAL VEHICLE FOLLOWING

Driver behavior in vehicle following has been an active area of research since the early 50's [2]–[6]. In vehicle following, the human driver acts as a controller. He senses velocities, distances, and accelerations and decides about control actions accordingly. In order to study these human control actions and their interaction with the vehicle dynamics, several investigators consider the development of mathematical models that mimic human driver behavior. The structure of one such mathematical model that was studied in literature is shown in Fig. 1.

Using the structure of Fig. 1, several investigators came up with mathematical equations that describe the input-output properties of each block in Fig. 1, leading to several human driver models described in the following subsections. These

models are based on vehicle following in a single lane with no passing.

A. Linear Follow-the-Leader Model

This model is based on vehicle-following theory, which pertains to single-lane dense traffic with no passing and assumes that each driver reacts in some specific fashion to a stimulus from the vehicle or vehicles ahead of him. The stimulus is the velocity difference, and the driver's response is an acceleration command to the vehicle. The block diagram of this model is shown in Fig. 2. Pipes first proposed this model in [4]. The dynamics of the vehicle are modeled by an integrator and the driver's central processing and neuromuscular dynamics by a constant. Chandler [5] used vehicle-following data to validate this model at the General Motors technical center. They showed experimentally that the reaction time was approximately 1.5 s and the constant gain K was approximately 0.37 sec^{-1} .

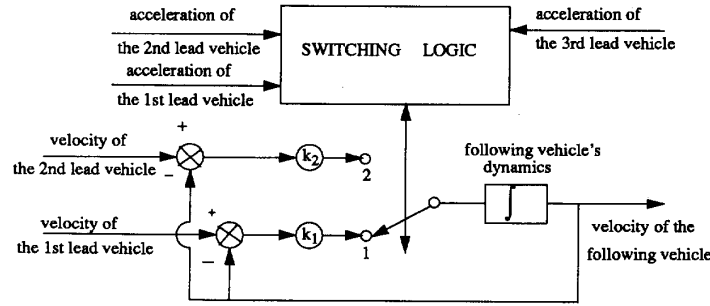


Fig. 4. Look-ahead model.

B. Linear Optimal Control Model

In [6] it is assumed that the human driver mimics a linear optimal controller in performing vehicle following. The optimal controller is based on a quadratic cost function that penalizes the weighted sum of the square of the inter-vehicle spacing and the square of the relative velocity. Since these weights differ from driver to driver and are, therefore, unknown, this optimal control approach can only be used to come up with the structure of the controller the human driver mimics. Another drawback of this approach is that it omits the driver's reaction time, the neuromuscular dynamics, and nonlinearities of the vehicle dynamics. For these reasons Burnham [2], [3] first modified the optimal controller structure by introducing the effects of the reaction time and vehicle nonlinearities and then estimated the unknown parameters and controller gains using real traffic data. The resulting model is shown in Fig. 3. The vehicle dynamics are modeled as

$$\dot{V}_F = u(t - \tau) - \rho V_F - \beta V_F^2$$

where V_F is the velocity of the vehicle in m/s; $u(t)$ is the acceleration command in m/sec^2 ; ρ is a coefficient related to mechanical drag in sec^{-1} ; β is a coefficient that depends on the aerodynamic drag in m^{-1} ; τ is the reaction time in sec . The initial condition $(S_L - S_F)(0)$ for the integrator in Fig. 3 represents the initial relative distance between the leading and following vehicle. In our simulations in Section IV, this distance is taken to be equal to one vehicle length plus some desired inter-vehicle spacing measured from the rear of the leading to the front of the following vehicle.

C. Look-Ahead-Model

This model [2], [3] is postulated on the hypothesis that the human driver observes the behavior of three vehicles directly ahead of him. The block diagram of this model is shown in Fig. 4. The switching logic operates to determine a majority direction of acceleration and then actuates the mode-switch accordingly. If the majority direction is the same as that of the first lead vehicle, it switches to position 1, (see Fig. 5). Otherwise, it operates at position 2. Typical parameter values obtained by fitting actual data are: $k_1 = 0.2sec^{-1}$ and $k_2 = 0.65sec^{-1}$.

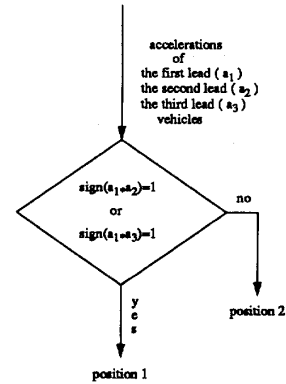


Fig. 5. Switching logic in Look-ahead Model.

III. AUTOMATED VEHICLE CONTROL

The human driver models considered in the previous section try to mimic the control actions of the driver with a certain controller. This controller is rather simple and consists of a delay that models the human driver reaction time. All models considered assume a simple model for the vehicle dynamics. This is not surprising, since most drivers treat the vehicle as a constant gain or at most as a first-order system with simple nonlinearities.

The human driver controller can be replaced with a more sophisticated one that is based on a more realistic model of vehicle dynamics and driven by a computer and physical sensors. Computer control will eliminate human reaction time, be more accurate, and be capable of achieving much better performance. Better performance will translate into smoother traffic flows, improved flowrate, less pollution, and safer driving.

A. Safety Distance Policy

The inter-vehicle distance dictated by the California rule is about a vehicle length for every 10 mph. For example, for an average vehicle length of about 15 ft. (i.e. about 4.5 meters), at 40 mph the safety distance is about 18 meters, and at 60 mph is about 27 meters. This safety distance policy takes into account the human driver reaction time in a rather conservative manner.

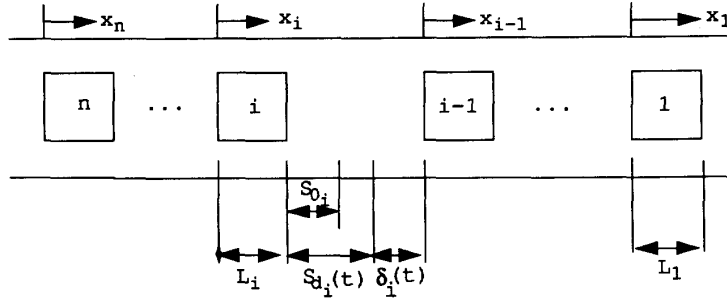
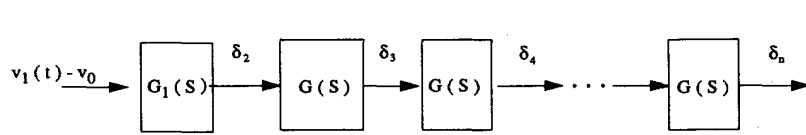
Fig. 6. A platoon of n vehicles with No. 1 being the lead vehicle.

Fig. 7. Block diagram of platoon dynamics.

With automation and good sensors, the human reaction time can be eliminated, and the safety distance between vehicles can be reduced considerably. In this section, we develop a safety distance policy that we employ in automatic vehicle following to be considered in the next section as follows: We consider an arbitrary vehicle-following situation, where the lead and following vehicle have the same acceleration and jerk constraints. For safe operation, we require the following vehicle to maintain sufficient safety distance throughout all maneuvers in order to avoid impact when the front vehicle suddenly executes a stop maneuver. The safety distance policy for each vehicle i is defined as

$$S_{d_i} \stackrel{\text{def}}{=} S_{m_i} + S_{a_i}$$

Where S_{m_i} is the minimum separation distance that the following vehicle should keep from the lead vehicle in order to avoid collision under some extreme stop situations. S_{a_i} is an additional gap for improved safety margins. The distance S_{d_i} is, therefore, defined as the rear-to-front desired vehicle spacing. One extreme stopping situation is the one where the lead vehicle is assumed to be at full negative acceleration ($-A_{\max}$) while the following vehicle is at fully positive acceleration (a_{\max}) at the instant the stop maneuver commences (i.e. at $t = t_0$, say). We assume that the maximum allowable jerk during acceleration is J_{\max} and develop (see Appendix A) the following expression for S_{m_i}

$$\begin{aligned} S_{m_i} = & \frac{v_i^2 - v_{i-1}^2}{2A_{\max}} + v_i \left(T + \frac{a_{\max} + A_{\max}}{J_{\max}} \right. \\ & + \frac{1}{A_{\max}} \left(a_{\max} T + \frac{a_{\max}(a_{\max} + A_{\max})}{J_{\max}} \right. \\ & \left. \left. - \frac{1}{2} \frac{(a_{\max} + A_{\max})^2}{J_{\max}} \right) \right) \\ & + \left(\frac{1}{2} a_{\max} T^2 + \frac{a_{\max}(a_{\max} + A_{\max})^2}{2J_{\max}^2} \right. \\ & \left. - \frac{1}{6} \frac{(a_{\max} + A_{\max})^3}{J_{\max}^2} + \frac{a_{\max}(a_{\max} + A_{\max})}{J_{\max}} T \right) \end{aligned}$$

$$\begin{aligned} & + \frac{1}{2A_{\max}} \left(a_{\max} T + \frac{a_{\max}(a_{\max} + A_{\max})}{J_{\max}} \right. \\ & \left. - \frac{1}{2} \frac{(a_{\max} + A_{\max})^2}{J_{\max}} \right)^2 \end{aligned} \quad (1)$$

where v_{i-1}, v_i are the velocities of the lead and following vehicle respectively at $t = t_0$, and T is the time required to detect the onset of the stopping maneuver initiated by the lead vehicle. In the human driver, model T depends on the human reaction time, whereas in the automatic case, T represents sensor communication delays due to sampling, etc.

Using (1) the expression for the safety distance policy becomes

$$S_{d_i} = \lambda_1(v_i^2 - v_{i-1}^2) + \lambda_2 v_i + \lambda_3 \quad (2)$$

for some constants $\lambda_1, \lambda_2, \lambda_3$. For tight vehicle following (i.e. v_i is close to v_{i-1}) expression (2) becomes

$$S_{d_i} = \lambda_2 v_i + \lambda_3. \quad (3)$$

The safety distance rule (3) combines the constant time headway rule ($S_{d_i} = \lambda_2 v_i$) with the constant separation rule ($S_{d_i} = \lambda_3$).

The California rule can be expressed as $S_{d_i} = \lambda_2 v_i$ where v_i is in m/s and λ_2 is in sec. Using the spacing of one vehicle length L in meters for every 10 m.p.h. we have

$$S_{d_i} = \lambda_2 v_i = \frac{v_i}{10} L \frac{3600}{1600} = 0.225 L v_i$$

which gives that the California constant time headway is $\lambda_2 = 0.225 L$ s.

The California rule is a rule of thumb suggested for human driving, and it, therefore, involves human reaction times and delays. In automatic vehicle following, human delays are eliminated, and in principle we can afford to have a time headway smaller than $0.225 L$ sec without affecting safety.

Using some suggested values for J_{\max} and a_{\max} given in [10] [14], i.e. $J_{\max} = 76.2 \text{ m/s}^3$, $a_{\max} = 3.92 \text{ m/s}^2$ (0.4 g)

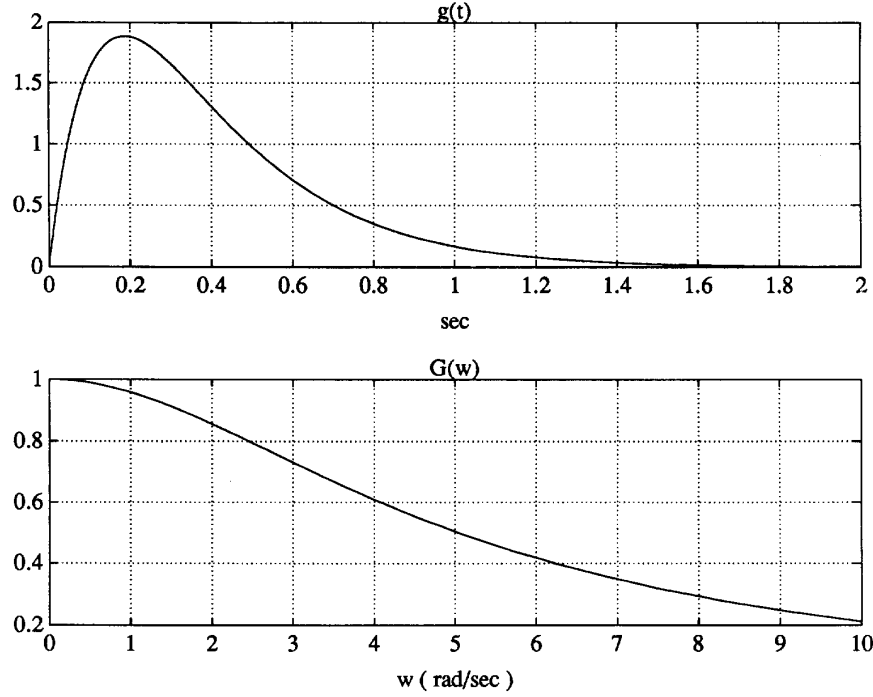


Fig. 8. The impulse response and magnitudes of frequency response.

and $A_{max} = 7.84 \text{ m/s}^2$ (0.8 g) the time headway λ_2 is about 0.12 s by assuming that $T = 0$. In reality, T will account for communication delays between sensors and will be small but nonzero. The VORAD radar sensor [13] provides relative speed and distance measurements every 0.1 s. Setting $T = 0.1$ s and using (1) we obtain $\lambda_2 = 0.27, \lambda_3 = 0.08$ m. This analysis suggests that a constant time headway of $\lambda_2 \geq 0.3$ s may be a safe rule for vehicle following. Shorter spacing can be achieved if the sampling period and accuracy of the ranging sensor is improved further.

B. Automatic Vehicle Following

1) *Vehicle Model:* In this report, we adopt the following model for the i_{th} vehicle in a platoon of vehicles in a lane proposed in [1].

$$\frac{d}{dt}x_i(t) = \dot{x}_i(t) = v_i(t) \tag{4}$$

$$\frac{d}{dt}\dot{x}_i(t) = \ddot{x}_i(t) = a_i(t) \tag{5}$$

$$\frac{d}{dt}\ddot{x}_i(t) = b(\dot{x}_i, \ddot{x}_i) + \alpha(\dot{x}_i)u_i(t) \tag{6}$$

where

$$\alpha(\dot{x}_i) = \frac{1}{m_i\tau_i(\dot{x}_i)}$$

$$b(\dot{x}_i, \ddot{x}_i) = -2\frac{k_{d_i}}{m_i}\dot{x}_i\ddot{x}_i - \frac{1}{\tau_i(\dot{x}_i)}\left[\ddot{x}_i + \frac{k_{d_i}}{m_i}\dot{x}_i^2 + \frac{d_{m_i}(\dot{x}_i)}{m_i}\right]$$

- x_i is the position of the i_{th} vehicle in meters.
- v_i is the velocity of the i_{th} vehicle in m/s.
- a_i is the acceleration of the i_{th} vehicle in m/s^2 .
- m_i is the mass of the i_{th} vehicle in kg.
- τ_i is the i_{th} vehicle's engine time constant in s.
- $u_i(t)$ is the i_{th} vehicle's engine input.
- k_{d_i} is the aerodynamic drag coefficient of the i_{th} vehicle in kg/m .
- $d_{m_i}(\dot{x}_i)$ is the mechanical drag of the i_{th} vehicle in kg m/s^2 which is a nonzero-constant but zero for zero velocity.

The configuration of a platoon of n vehicles is shown in Fig. 6.

- In Fig.6 L_i denotes the length of the i_{th} vehicle in meters.
- $S_{d_i}(t)$ is the desired safety spacing in meters.
- $S_{o_i} = S_{d_i}(t_0)$ is the spacing at initial time $t = t_0$.
- $\delta_i(t)$ is the deviation from the desired safe spacing. It can have positive or negative values.

2) *Autonomous Intelligent Cruise Control Law:* In an AICC system each vehicle is assumed to be able to measure

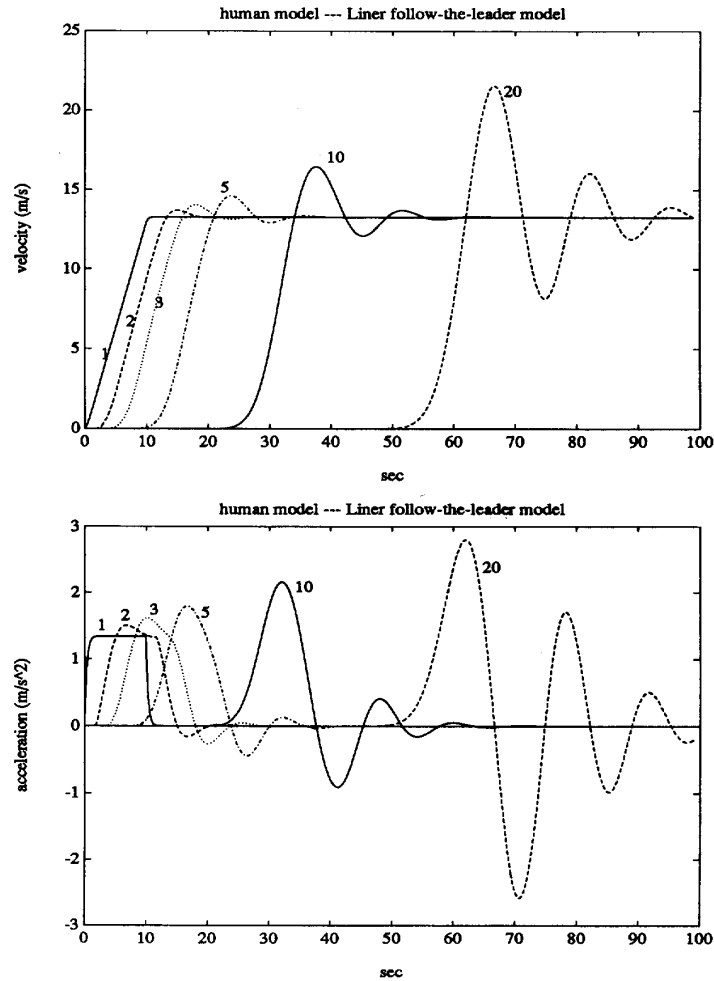


Fig. 9. Transient response of human driver vehicle following (Pipes Model).

the relative distance and relative velocity between itself and the immediate front vehicle in addition to its own velocity and acceleration. Based on these measurements and the safety distance rule $S_{d_i} = \lambda_2 v_i + S_{O_i}$ and motivated from the results of [1] which were developed for constant spacing, i.e. $S_{d_i}(t) = \lambda_3$, we propose the following control law:

$$u_i(t) = \frac{1}{\alpha(\dot{x}_i)} [c_i(t) - b(\dot{x}_i, \ddot{x}_i)] \quad (\text{for } i = 2, 3, 4, \dots, n) \quad (7)$$

where

$$\begin{aligned} c_i(t) &= C_p \delta_i(t) + C_u \dot{\delta}_i(t) \\ &\quad + K_v v_i(t) + K_a a_i(t) \\ \delta_i(t) &= x_{i-1}(t) - x_i(t) \\ &\quad - (L_i + S_{O_i} + \lambda_2 v_i(t)) \end{aligned} \quad (8)$$

$$\begin{aligned} \dot{\delta}_i(t) &= v_{i-1}(t) - v_i(t) \\ &\quad - \lambda_2 a_i(t) \\ &\quad (\text{for } i = 2, 3, \dots, n) \end{aligned} \quad (9)$$

and C_p, C_v, K_v, K_a are design constants. Using (7) in (4)–(6), the closed-loop dynamics of the vehicle following system with initial conditions: $v_i(0) = v_0$ and $\delta_i(t) = \dot{\delta}_i(t) = \ddot{\delta}_i(t) = 0$ for $i = 2, 3, \dots, n$ are described by the linear system of Fig. 7, where

$$G_1(s) = \frac{s^2 - K_a s - K_v}{F(s)} \quad (10)$$

$$G(s) = \frac{C_v s + C_p}{F(s)} \quad (11)$$

$$\begin{aligned} F(s) &= s^3 + (\lambda_2 C_v - K_a) s^2 \\ &\quad + (C_v + \lambda_2 C_p - K_v) s + C_p \end{aligned} \quad (12)$$

In Fig. 7 the constants C_p, C_v, K_v and K_a are to be chosen to meet the following four design considerations:

1. For stability we require the poles of $G_1(s)$ and $G(s)$ to be in the open left s -plane.
2. For steady-state performance we require $\delta_i(t) \rightarrow 0$ as $t \rightarrow \infty$.

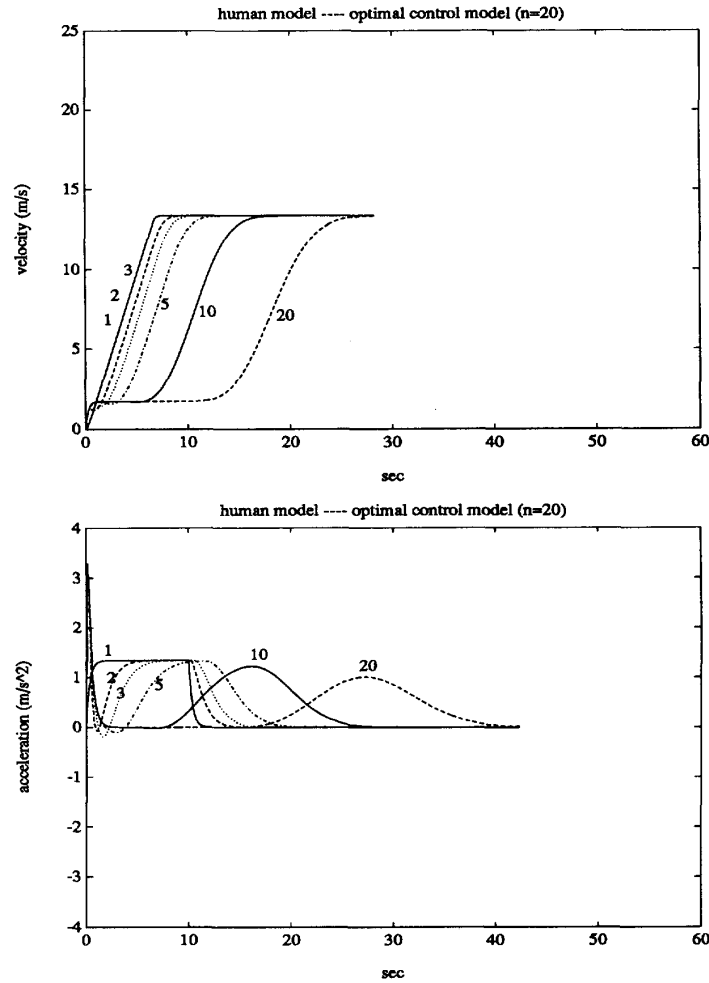


Fig. 10. Transient response of human driver vehicle following (Optimal Model).

3. In order to avoid slinky-type effects [1, 2, 11] we require $|G(jw)| < 1$ for all $w > 0$.
4. In order to avoid an oscillatory behavior in $\delta_i(t)$ [1] we require the impulse response $g(t)$ of $G(s)$ to satisfy $g(t) > 0$ for all $t > 0$.

It is clear from (11) that the stability Constraint 1 can be easily achieved by choosing the various constants. Constraint 2 is also satisfied by choosing $K_v = 0$. Constraint 3 requires $|G(jw)| < 1$ for all $w > 0$ in order to avoid the slinky-type effects. The slinky-type phenomenon is well known in vehicle following without feedforward information in the case of human driver models [2] and automatic vehicle following with constant spacing [1]. The lack of information about the actions of the lead vehicle causes a disturbance amplification in the values of deviation δ_i , velocities, and accelerations of the following vehicles.

The significance of our approach lies in the ability to eliminate the slinky phenomenon by using the constant time headway safety rule. This rule provides the additional freedom that allows us to achieve $|G(jw)| < 1$ for all $w > 0$ by

designing the control system appropriately as explained below in (13), shown at the bottom of the page.

We require

$$|G(jw)|^2 = \frac{C_p^2 + C_v^2 w^2}{[C_p - (\lambda_2 C_v - K_a)w^2]^2 + w^2[(C_v + \lambda_2 C_p - K_v) - w^2]^2} < 1, \quad \forall w > 0 \quad (13)$$

Choosing $K_v = 0$ and substituting it into (13), we obtain the following inequality:

$$w^4 + [(\lambda_2 C_v - K_a)^2 - 2(C_v + \lambda_2 C_p)]w^2 + (\lambda_2^2 C_p + 2K_a)C_p > 0, \quad \forall w > 0. \quad (14)$$

For constant spacing separation policy (i.e., $\lambda_2 = 0$), the inequality (14) reduces to

$$w^4 + (K_a^2 - 2C_v)w^2 + 2K_a C_p > 0, \quad \forall w > 0. \quad (15)$$

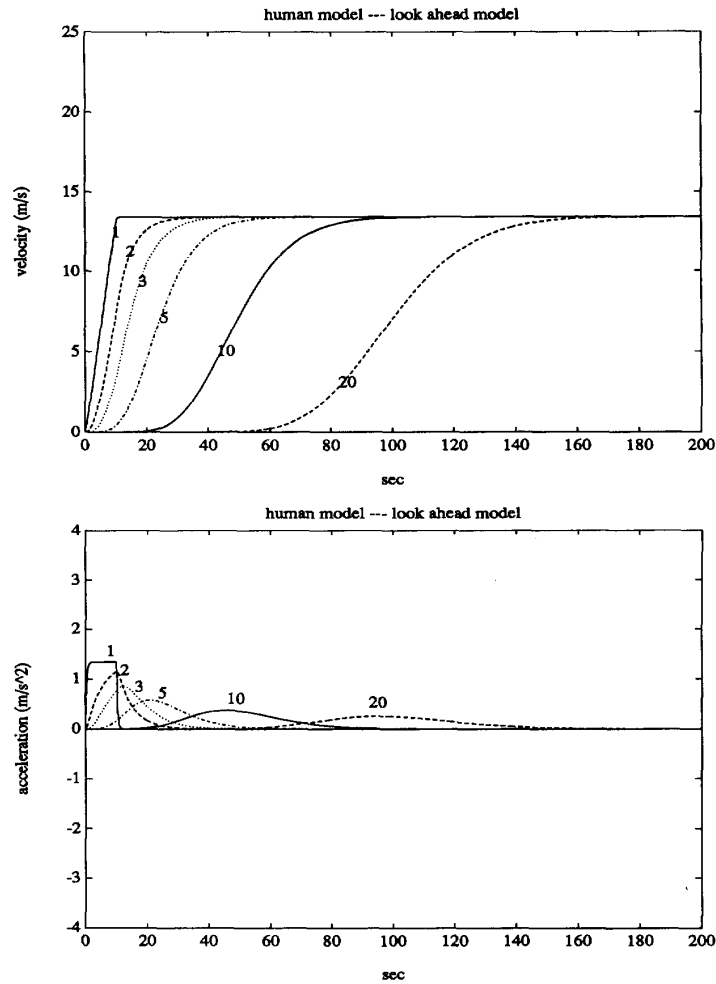


Fig. 11. Transient response of human driver vehicle following (Look-ahead Model).

For $\lambda_2 = 0$, $F(s) = s^3 - K_a s^2 + (C_v - K_v)s + C_p$. To ensure closed loop stability, C_p should be chosen positive, and K_a should be chosen negative. Therefore, the term $K_a C_p$ in inequality (15) is always negative. This implies that the inequality (15) cannot be satisfied for all $w > 0$. Thus the slinky-type effects can not be avoided when $\lambda_2 = 0$. However, for constant time headway safety policy, if we choose λ_2, K_a and C_p such that $\lambda_2^2 C_p^2 + 2K_a C_p \geq 0$ and $(\lambda_2 C_v - K_a)^2 \geq 2(C_v + \lambda_2 C_p)$, then the inequality (14) is satisfied for all $w > 0$, and hence the slinky-type effects can be avoided.

The fourth design consideration is that $g(t) > 0$ for $t > 0$ where $g(t)$ is the impulse response of $G(s)$. The condition $g(t) > 0$ guarantees the lack of oscillations in the deviations $\delta_i(t)$ as explained in [1]. If we choose the design constants; $C_p = 4, C_v = 28, K_v = 0, K_a = -0.04$, the impulse and frequency responses demonstrate the lack of slinky effects ($|G(jw)| < 1$) and reduction in oscillations as shown in Fig. 8 ($g(t) > 0$ most of the time). Since $g(t)$ is not greater than or equal to zero at all times, oscillations cannot be

completely eliminated. Since $|G(jw)| < 1$ for all frequencies, the amplitude of these oscillations, however, is attenuated considerably downstream the traffic flow as is clear from Fig. 7. Their effect is, therefore, negligible as demonstrated in the next section by simulations.

Remark 1: In a practical situation, the design considerations 1 to 4 should be augmented with another one that limits the maximum acceleration, deceleration, and jerk, in order to achieve riding comfort. Without these constraints, the control law may produce high control power in situations where large position or velocity errors are present. High power control may make riding uncomfortable and jerky. In this paper, we have not addressed these situations, and, therefore, we didn't consider this problem. This problem, however, is addressed and resolved in [12], [16].

Remark 2: The choice of the control law in (7) follows directly from the theory of feedback linearization [15] where one part of the control action is used to cancel the nonlinearities, and the other part is used to assign the eigenvalues of the resulting linear system.

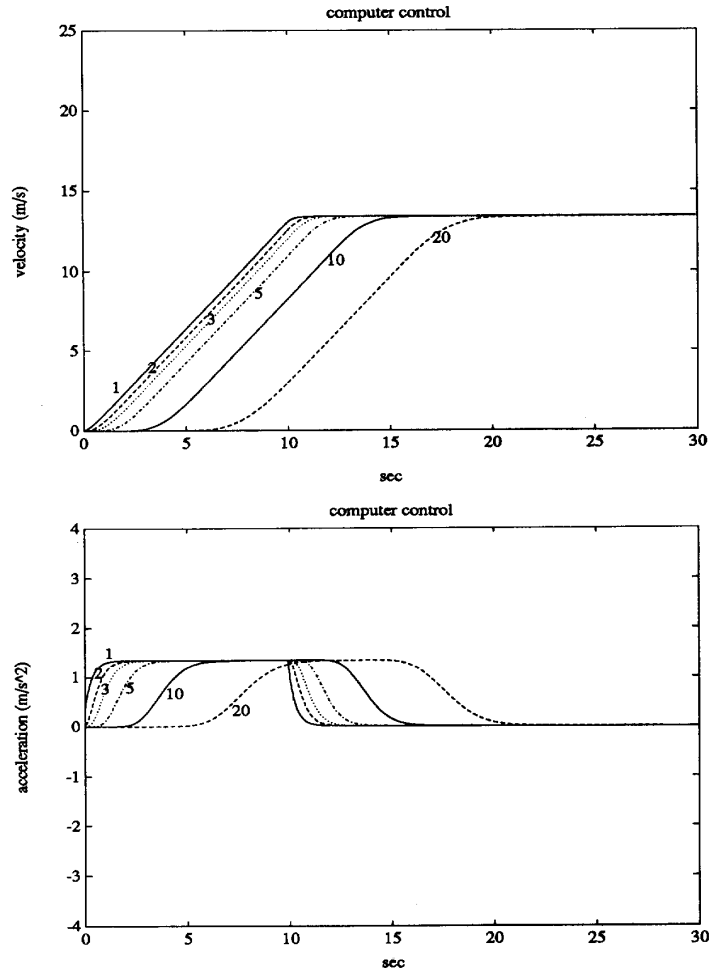


Fig. 12. Transient response of automatic vehicle following.

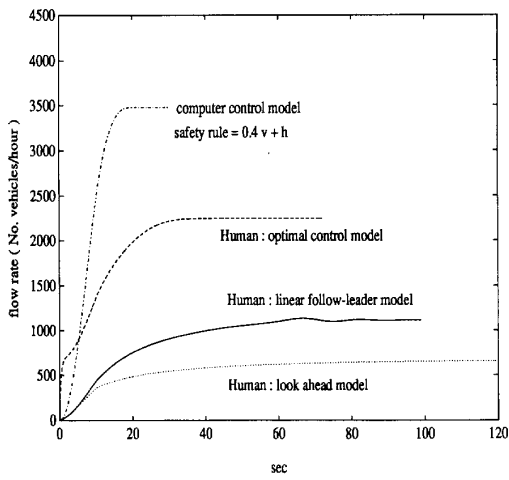


Fig. 13. Transient traffic flow rate ($h = 4$ m to 4.5 m).

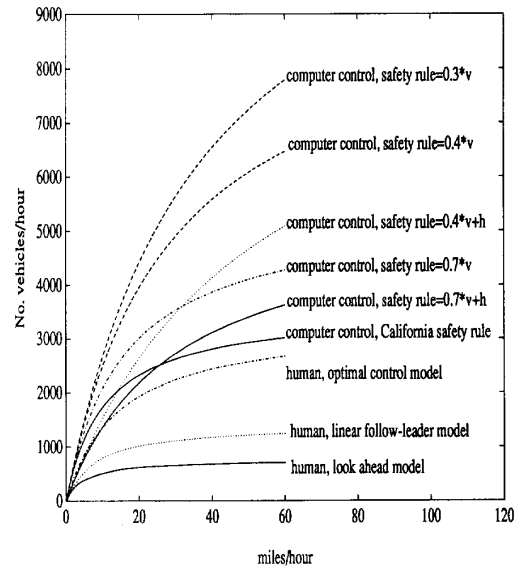


Fig. 14. Steady-state traffic flow rate versus steady-state speed ($h = 4$ m to 4.5 m).

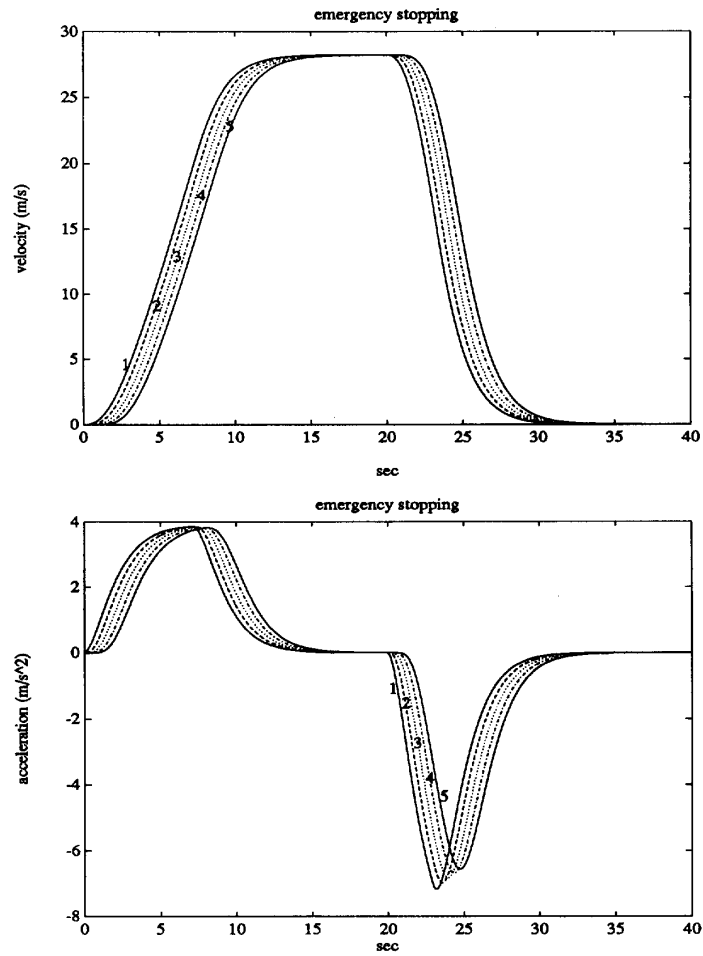


Fig. 15. Emergency stopping response (velocity and acceleration).

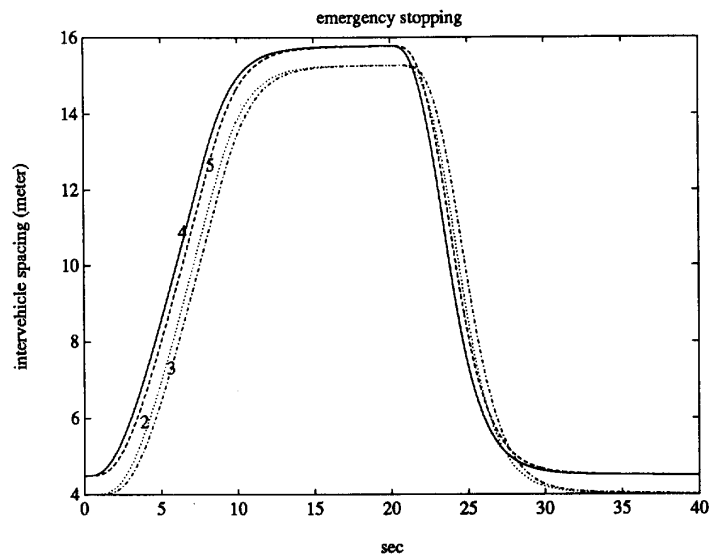


Fig. 16. Inter-vehicle spacing during an acceleration and stopping maneuver for vehicle 2, 3, 4, and 5.

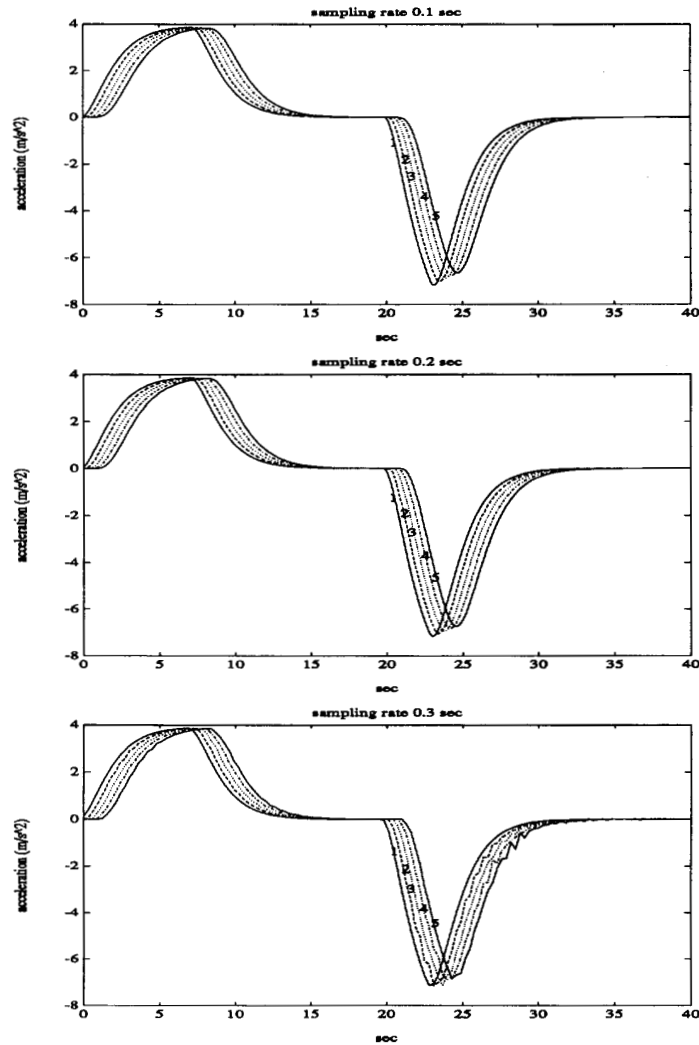


Fig. 17. Effect of sampling period of ranging sensor on acceleration responses for vehicles 1, 2, 3, 4, and 5.

IV. SIMULATIONS

We consider $2n$ vehicles following each other in a single lane with no passing. The length of vehicles is assumed to be $L_i = 4.5$ m to 5 m, i.e. n vehicles are assumed to be of length 5 m and n of length 4.5 m. Automatic vehicle following with the safety distance separation rule $S_{d_i} = \lambda_2 v_i + \lambda_3$ in meters, where λ_2, λ_3 are to be chosen, is simulated. We assume the initial condition $S_{d_i}(0) = \lambda_3 = 4$ to 4.5 m. We also assume that the maximum acceleration, maximum jerk (accelerating), maximum deceleration, and maximum jerk (decelerating) are 4 m/s^2 , 3 m/s^3 , 8.0 m/s^2 and -75 m/s^3 , respectively. The desired spacing for the human driving in optimal control model is assumed to be 1.5 m. Using the same constants as in [1], we assume that the mass of the first n vehicles is 2000 kg, and the mass of the other n vehicles is 1800 kg; the aerodynamic drag coefficient of the first n vehicle is 0.51 kg/m and 0.45 kg/m for the other n vehicles. The mechanical drag for all $2n$ vehicles is assumed to be 4 kg

m/s^2 , and engine time constant are 0.25 s and 0.3 s for the first n and the rest of the vehicles, respectively. We perform the following tests:

Test 1: Transient Behavior:

We assume that the lead accelerates from 0 speed to 30 mph (13.4 m/s) and n is equal to 10. The velocity and acceleration responses versus time of the human driver models are shown in Figs. 9–11. The slinky effects and oscillations are very pronounced in the Pipes model. The optimal control model shows no slinky effect but small initial oscillations and large transience in acceleration of some of the vehicles. The look-ahead model, due to the feedforward information it assumes, shows no slinky effects or oscillations and does not experience large accelerations. The steady state is reached after 120 s in the case of Pipe's model, in about 40 s in the case of the optimal model, and in about 160 s in the look-ahead model. As a result, the traffic flow measured in number of vehicles/hour varies among the human driver models as shown in Fig. 13.

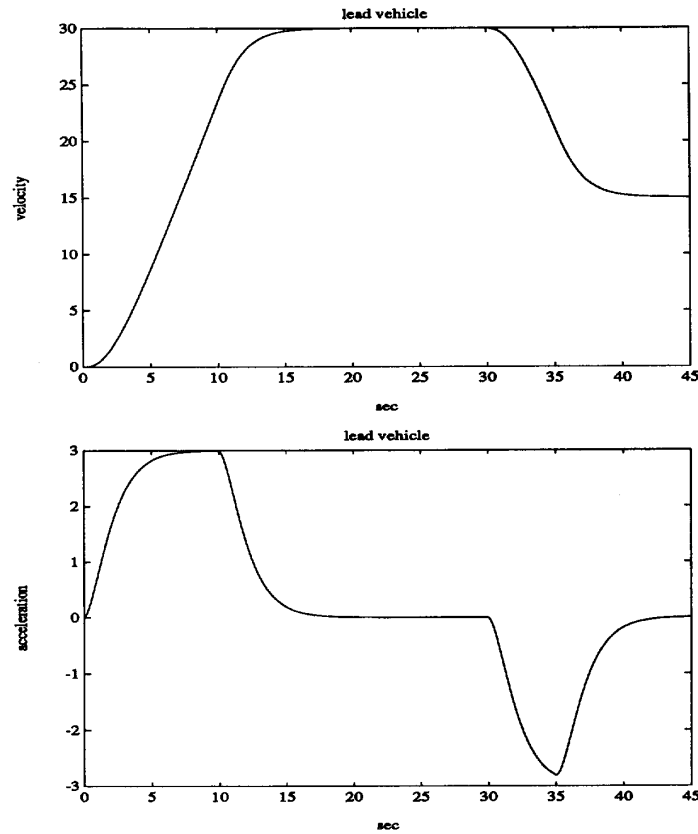


Fig. 18. The velocity and acceleration responses of the lead vehicle during the test of cut-in situations.

The response of the automatic vehicle following is shown in Fig. 12 for $\lambda_2 = 0.4$ s and $\lambda_{3_i} = 4$ m or 4.5 m for the various vehicles. It is clear that no slinky effects and oscillations are present and steady state is reached much faster, i.e. in about 15 s. The traffic flow rate in this case is much higher than any of the three human driver models due to the faster response and the safety rule of $\lambda_2 = 0.4$ s, $\lambda_{3_i} = 4$, or 4.5 m that allows closer inter-vehicle spacing at steady state than those assumed by the human driver models.

Test 2: Steady State Performance:

In this test, we examine the effect of human driver and automatic vehicle following on the traffic flow rate at different steady state speeds. We assume n is 10. The results of the simulations are shown in Fig. 14. It is clear that automatic vehicle following leads to much higher traffic flow rates due to the smaller inter-vehicle spacings. However, even with the California rule spacing, an improvement of 12% over the best human driver model is achieved due to the elimination of human delays and slow reaction time. We should emphasize that these results are obtained for vehicles in a single lane with no passing. In the case of multiple lanes with lane changing, the results shown in Fig. 14 will have to be modified.

Test 3: Emergency Stopping:

In this test, we simulated an emergency situation where the lead vehicle initially accelerates from 0 to 60 mph with

maximum acceleration of about 0.4 g, keeps a constant speed of 60 mph, and all of a sudden executes a stop maneuver using maximum deceleration of about 0.8 g. The simulation results showing distance, velocity, acceleration, and inter-vehicle spacing responses are shown in Fig. 15 and 16. All five vehicles simulated came to a full stop in about 10 s, since the initiation of the stop maneuver, with no collision. The safety distance used for vehicle interspacing was $S_{d_i} = \lambda_2 v_i + S_{O_i}$ with $\lambda_2 = 0.4$ s and $S_{O_i} = 4$ m and 4.5 m.

Test 4: Robustness With Respect to Sensor Measurements:

In this test, we examined the effect of sampled sensor measurements on the performance of the AICC. We assumed that a radar sensor is used for relative distance and relative velocity measurements, providing information at a rate of 10 Hz, 5 Hz, or 3.33 Hz; i.e., it has a sampling period of 0.1 s, 0.2 s, or 0.3 s. We used this sampling rate to repeat test 3, the emergency stopping case. The results are shown in Fig. 17. It is clear that the control law and safety distance rule used are robust with respect to the sensor sampling rate of 10 Hz, 5 Hz and 3.3 Hz.

Test 5: Cut-in Situation:

An important emergency situation pointed out by several researchers from the automobile industry [14] is the cut-in situation. In this case, a vehicle that is manually driven cuts between a number of vehicles which are automatically driven us-

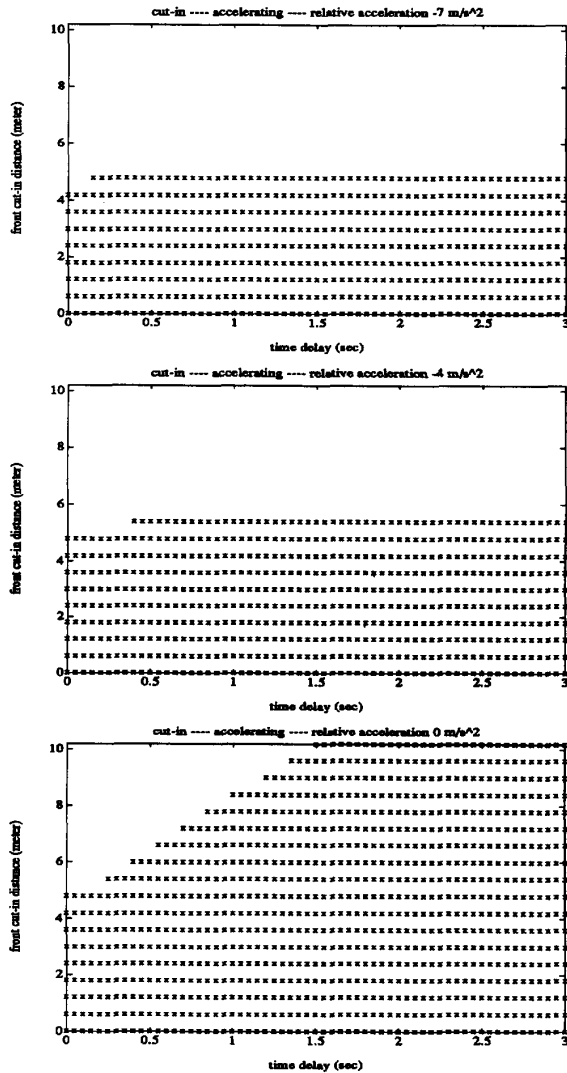


Fig. 19. Dotted region is where collision will take place between cut-in vehicle and vehicle in front.

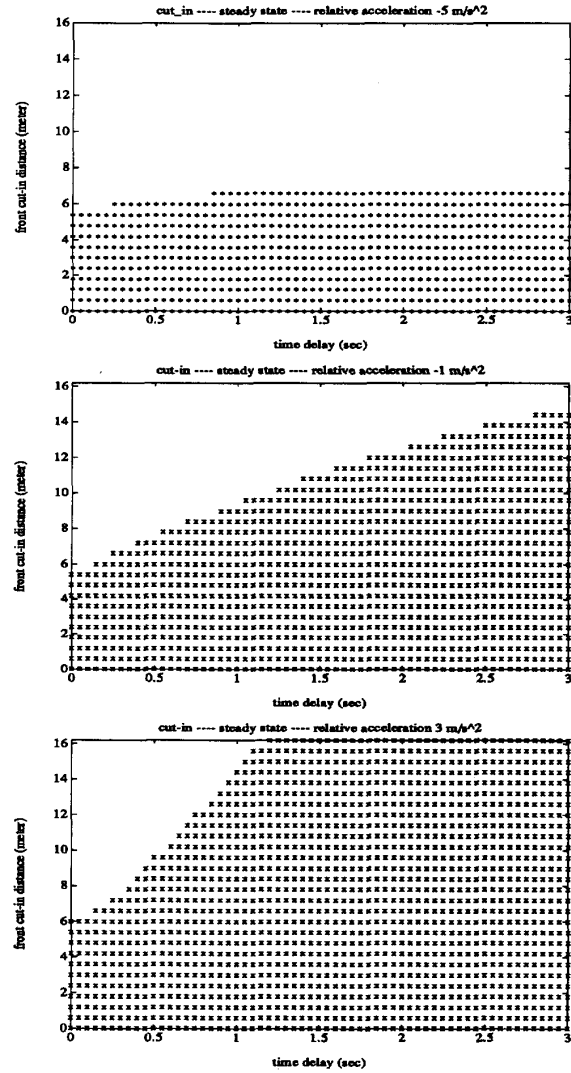


Fig. 20. Dotted region is where collision will take place between cut-in vehicle in front.

ing the AICC. The intention of the cut-in vehicle is to join the string of vehicles already operating on AICC and switch from manual to AICC mode. The purpose of this test is to examine various cut-in situations and find the conditions under which collisions can be avoided. It is clear that if the cut-in vehicle violates the safety distance rule, then collision cannot be avoided under some situations of rapid accelerations or decelerations of the various vehicles involved. We consider the following situation: The lead vehicle accelerates from 0 to 30 m/s, keeps a constant speed of 30 m/s for awhile, and then decelerates to 15 m/s as shown in Fig. 18. We assume that the total number of vehicles is six, and the cut-in vehicle cuts in between the second vehicle and the following one. The cut-in vehicle switches to the AICC mode as soon as it cuts in with some delay. We assume that the velocity of the cut-in vehicle is initially higher than that of the vehicles on the AICC mode. We consider the following three cases: The cut-in vehicle cuts in when (1)

vehicles on AICC are accelerating, (2) vehicles on AICC are at constant speed, and (3) vehicles on AICC are decelerating. In each of the above cases, we assume two subcases. In the first one, the cut-in vehicle has a higher velocity and acceleration than the vehicle behind, and in the second subcase, the cut-in vehicle has a higher velocity but lower acceleration than the vehicle behind. The cut-in times are $t = 10$ s (case (1) above), $t = 20$ s (case (2) above) and $t = 32$ s (case (3) above). We define the front cut-in distance as the spacing between the cut-in vehicle and the vehicle in front and the rear cut-in distance as the spacing between the cut-in vehicle and the vehicle behind.

The simulation results are shown in Fig. 19 to 21. The curves show the response versus time delay for switching to the AICC mode at various different initial accelerations of the cut-in vehicle, whose initial velocity is 5 mph higher than that of the vehicle behind. The dotted region is the region

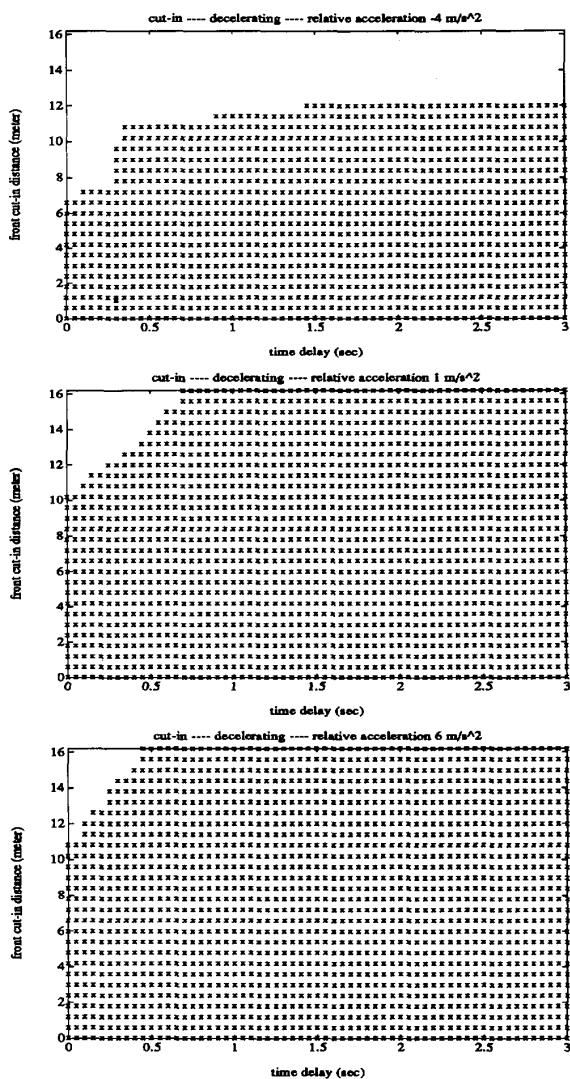


Fig. 21. Dotted region is where collision will take place between cut-in vehicle and vehicle in front.

where the cut-in vehicle will collide with the vehicle in front. Our results show that no collision will take place between the cut-in vehicle and the vehicle behind under the conditions considered. This is due to the fact that the initial velocity of the cut-in vehicle is assumed to be 5 mph higher than that of the vehicle behind (a reasonable assumption) which implies that the safety distance rule becomes satisfied in a very short interval of time.

Collisions, however, will occur between the cut-in vehicle and vehicle in front depending on the cut-in distance and time delay of switching to the AICC mode as shown by the dotted region of Figs. 19–21. Further tests and analysis are necessary in order to understand and quantify all possible collision cases.

Test 6: Exit from the AICC Mode:

In this case, we simulated the situation where a vehicle terminates automatic vehicle following by exiting to a lane

with manual vehicle following. The exit operation is simulated to take place at $t = 8$ s when vehicles are in an accelerating mode as shown in Fig. 22. Seven vehicles are simulated, and the third vehicle is assumed to exit the automatic lane. As shown in Fig. 22, the exiting vehicle causes some change in the inter-vehicle spacing that is soon accommodated by the following vehicles.

V. CONCLUSION

The focus of this study was on vehicle following in a single lane under the assumption that all vehicles use a proposed autonomous intelligent cruise control system (AICC) to do vehicle following. Automatic vehicle following is compared with a manual one modeled by three different human driver models proposed in literature. This comparison indicates a strong potential for AICC to smooth traffic flows and increase traffic flow rates considerably if designed and implemented properly. Several emergency situations were simulated and used to demonstrate that the AICC proposed may lead to much safer driving.

ACKNOWLEDGMENT

The authors would like to thank J. Hauser, Z. Xu, M. Shulman, E. Farber, and S. Sheikholeslam for many helpful discussions on the subject of vehicle following.

APPENDIX A SAFETY DISTANCE POLICY:

The minimum safety separation safety distance S_{m_i} between the two vehicles may be expressed as

$$S_{m_i} = D_i - D_{i-1} \quad (A.1)$$

where D_{i-1} is the stopping distance of the front vehicle ($i-1$) with initial velocity $v_{i-1}(t_0)$ and $a_{i-1}(t_0) = -A_{\max}$ and D_i is the stopping distance of vehicle i with velocity $v_i(t_0)$ and initial acceleration $a_i(t_0) = a_{\max}$. The time t_0 is the initial time that a stopping maneuver starts. (Without loss of generality, we assume $t_0 = 0$).

The situation considered is the one where vehicle ($i-1$) decelerates as

$$a_{i-1}(t) = -A_{\max} \quad 0 \leq t \leq \frac{v_{i-1}(0)}{A_{\max}}$$

and vehicle i follows with (as shown in Fig. 23)

$$\begin{aligned} a_i(t) &= a_{\max} & 0 \leq t \leq T & \text{(interval 1)} \\ &= a_{\max} - J_{\max}t & T \leq t \leq T + t_1 & \text{(interval 2)} \\ &= -A_{\max} & T + t_1 \leq t \leq T + t_1 + t_f & \text{(interval 3)} \end{aligned}$$

where T is the time required by vehicle to start the stopping maneuver. The time t_1 is the time required to reach a deceleration of $-A_{\max}$ from a_{\max} under the constraint of maximum jerk J_{\max} . The time t_1 is given by $t_1 = (a_{\max} + A_{\max})/J_{\max}$. The time t_f is the time at which vehicle i reaches a full stop (i.e. $v_i(T + t_1 + t_f) = 0$).

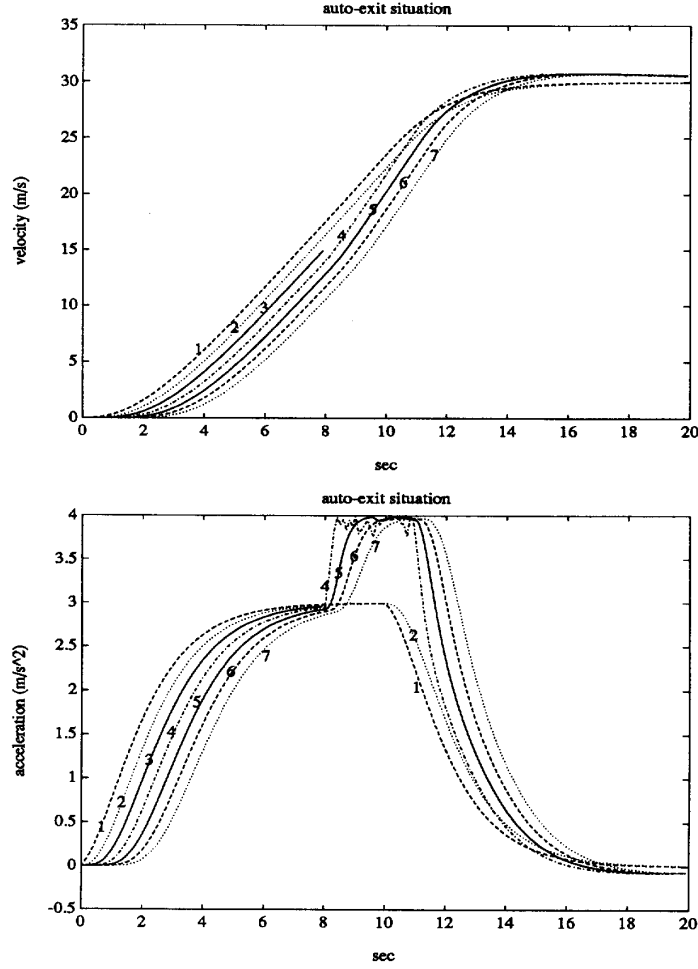


Fig. 22. Velocity and acceleration responses when vehicle No. 3 exits the automatic vehicle following lane at $t = 8$ s.

The stopping distance of vehicle $i - 1$ and i can be determined as

$$D_{i-1} = \frac{v_{i-1}^2(0)}{2A_{\max}}. \quad (\text{A.2})$$

We express D_i as

$$D_i = D_{1i} + D_{2i} + D_{3i} \quad (\text{A.3})$$

where D_{ji} is the stopping distance of vehicle i during the time interval j ($j = 1, 2, 3$) given

$$D_{1i} = \frac{v_i^2(T) - v_i^2(0)}{2a_{\max}} \quad (\text{A.4})$$

$$\begin{aligned} D_{2i} &= \int_0^{t_1} \left[v_i(t) + \int_0^t (a_{\max} - J_{\max} t) dt \right] dt \\ &= v_i(t) t_1 + \int_0^{t_1} \left(a_{\max} t - \frac{1}{2} J_{\max} t^2 \right) dt \\ &= v_i(t) t_1 + \frac{1}{2} a_{\max} t_1^2 - \frac{1}{6} J_{\max} t_1^3 \end{aligned} \quad (\text{A.5})$$

$$D_{3i} = \frac{v_i^2(T + t_1 + t_f) - v_i^2(T + t_1)}{-2A_{\max}}$$

$$= \frac{v_i^2(T + t_1)}{2A_{\max}}. \quad (\text{A.6})$$

The velocity $v_i(T)$ and $v_i(T + t_1)$ is given by

$$v_i(T) = v_i(0) + \int_0^T a_i(t) dt = v_i(0) + a_{\max} T \quad (\text{A.7})$$

$$\begin{aligned} v_i(T + t_1) &= v_i(T) + \int_0^T (a_{\max} - J_{\max} t) dt \\ &= v_i(0) + a_{\max} T + a_{\max} t_1 - \frac{1}{2} J_{\max} t_1^2 \end{aligned} \quad (\text{A.8})$$

Substituting (A.4)–(A.8) into (A.3), we can obtain (A.9), shown at the bottom of the page.

$$\begin{aligned} D_i &= \frac{v_i^2(0)}{2A_{\max}} + v_i(0) \left(T + \frac{a_{\max} + A_{\max}}{J_{\max}} \right. \\ &\quad \left. + \frac{1}{A_{\max}} \left(a_{\max} T + \frac{a_{\max}(a_{\max} + A_{\max})}{J_{\max}} \right) \right. \\ &\quad \left. - \frac{1}{2} \frac{(a_{\max} + A_{\max})^2}{J_{\max}} \right) \end{aligned}$$

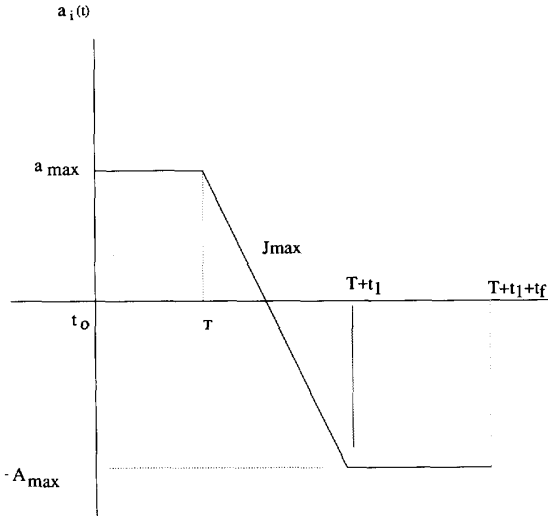


Fig. 23. Acceleration profile of vehicle i under a worst stopping scenario.

$$\begin{aligned}
 & + \left(\frac{1}{2} a_{\max} T^2 + \frac{a_{\max}(a_{\max} + A_{\max})^2}{2J_{\max}^2} \right. \\
 & - \frac{1}{6} \frac{(a_{\max} + A_{\max})^3}{J_{\max}^2} \\
 & + \frac{a_{\max}(a_{\max} + A_{\max})}{J_{\max}} T \\
 & + \frac{1}{2A_{\max}} \left(a_{\max} T + \frac{a_{\max}(a_{\max} + A_{\max})}{J_{\max}} \right. \\
 & \left. \left. - \frac{1}{2} \frac{(a_{\max} + A_{\max})^2}{J_{\max}} \right)^2 \right) \quad (A.9)
 \end{aligned}$$

The expression for S_{m_i} follows by substituting for D_i, D_{i-1} from (A.2), (A.9) to (A.1).

REFERENCES

- [1] S. Sheikholeslam, "Control of a class of interconnected nonlinear dynamical system: the platoon problem," Ph.D. dissertation, University of California, Berkeley, 1991.
- [2] G. O. Burnham, J. Seo, and G. A. Bekey, "Identification of human driver models in car following," *IEEE Trans. Automat. Cont.*, vol. 19, pp. 911-915, 1974.
- [3] G. A. Bekey, G. O. Burnham, and J. Seo, "Control theoretic models of human drivers in car following," *Human Factors*, vol. 19(4), pp. 399-413, 1977.
- [4] L. A. Pipes, "An operational analysis of traffic dynamics," *J. Applied Physics*, vol. 24, pp. 271-281, 1953.
- [5] F. E. Chandler, R. Herman, and E. W. Montroll, "Traffic dynamics: Studies in car following," *Operations Research*, vol. 6, pp. 165-184, 1958.
- [6] J. S. Tyler, "The characteristics of model following systems as synthesized by optimal control," *IEEE Trans. Automatic Control*, vol. AC-9, pp. 485-498.

- [7] D. E. Olson and W. L. Garrard, "Model follower longitudinal control for automated guideway transit vehicles," *IEEE Trans. Veh. Technol.*, vol. VT-28, Feb. 1979.
- [8] Research report by PROMETHEUS and personal communication with Dr. Mike Shulman, 1991.
- [9] S. J. Sklar, J. P. Bevans, and G. Stein, "Safe-approach vehicle-following control," *IEEE Trans. Veh. Technol.*, vol. 28, Feb. 1979.
- [10] R. E. Fenton, "A headway safety policy for automated highway operations," *IEEE Trans. Veh. Technol.*, vol. VT-28, Feb. 1979.
- [11] J. K. Hedrick, D. McMahon, V. Narendran, and D. Swaroop, "Longitudinal vehicle controller design for IVHS systems," *ACC*, pp. 3107-3112, 1991.
- [12] C. C. Chien and P. Ioannou, "Vehicle following controller design for autonomous intelligent vehicle," *Preprint*, 1993.
- [13] Personal communication with researchers from IVHS Technologies.
- [14] Personal communication with M. Shulman and E. Farber from Ford Motor Co.
- [15] A. Isidori, *Nonlinear Control Systems: An Introduction*. New York: Springer-Verlag, 1985.
- [16] P. Ioannou and Zhigang Xu, "Intelligent cruise control: Theory and experiment," submitted to *32nd CDC*, 1993.



Petros A. Ioannou was born in Cyprus on February 3, 1953. He received the B.Sc. degree with first class honors from University College, London, England, in 1978 and the M.S. and Ph.D. degrees from the University of Illinois, Urbana, Illinois, in 1980 and 1982, respectively.

From 1979 to 1982 he was a research assistant at the Coordinated Science Laboratory at the University of Illinois. In 1982, Dr. Ioannou joined the Department of Electrical Engineering-Systems, University of Southern California, Los Angeles, California. He is currently a Professor in the same Department and Director of the Center of Advanced Transportation Technologies. He teaches and conducts research in the areas of adaptive control, neural networks and intelligent vehicle and highway systems.

During the period 1975-1978, Dr. Ioannou held a Commonwealth Scholarship from the Association of Commonwealth Universities, London, England. He was awarded several prizes including the Goldsmid Prize and the A. P. Head Prize from University College, London. In 1984 Dr. Ioannou was a recipient of the Outstanding Transactions Paper Award for his paper, "An Asymptotic Error Analysis of Identifiers and Adaptive Observers in the Presence of Parasitics," which appeared in the IEEE TRANSACTIONS ON AUTOMATIC CONTROL in August 1982. Dr. Ioannou is also the recipient of a 1985 Presidential Young Investigator Award for his research in Adaptive Control. He has been an Associate Editor for the *IEEE Transactions on Automatic Control* from 1987 to 1990 and he is currently on the Editorial Board for the *International Journal of Control*. Dr. Ioannou is a member of IVHS America and the AVCS Committee of IVHS America.



C. C. Chien was born in Taiwan, Republic of China, on September 10, 1964. He is currently working toward the Ph.D. degree in the Department of Electrical Engineering-Systems, University of Southern California, Los Angeles.

His research interests are vehicle dynamics, control of nonlinear systems, adaptive control and traffic flow theory.